Journal of Hydroscience and Hydraulic Engineering
Vol. 7, No. 1, November, 1989, pp.23-34

LONGITUDINAL STRIPES OF SORTING DUE TO CELLULAR SECONDARY CURRENTS

By

Tetsuro TSUJIMOTO, Associate Professor

Department of Civil Engineering, Kanazawa University
2-40-20, Kodatsuno, Kanazawa, 920, JAPAN

SYNOPSIS

Longitudinal stripes of sorting is closely interrelated to cellular secondary currents, and they promote or suppress each other through a feed-back system of flow and sediment transport. In this paper, a reasonable model of heterogeneous size material transport is prepared, and the interrelation between fractional bed-load transport and secondary currents are carefully described.

A secondary currents causes a lateral bed-load transport from "rough" stripe to "smooth" stripe; and, if the finer material is predominantly transported laterally, alternate sorting is promoted. The condition of development of sorting is determined by the characteristics of bed-load motion for each grain size. Based on a phenomenological understanding of sorting and a reasonable bed-load transport model, a criterion of occurrence of longitudinal stripes due to alternate lateral sorting is clarified. Moreover, the spanwise distributions of composition of bed-surface layer and bed-load transport rate for equilibrium longitudinal stripes of sorting are also predicted.

INTRODUCTION

In a stream composed of sand and gravel, several kinds of sorting take place. Besides armor coat and pavement formation as monotonous sorting processes, "longitudinal stripes of sorting" and "diffuse gravel sheet" as cyclic sorting phenomena are interesting from the viewpoint of river morphology. These alternate sorting phenomena are also important from the view point of river engineering, because they often cause severe fluctuations of sediment discharge.

In a stream composed of sand and gravel, longitudinal stripes of bed-surface gradation or the transverse repetition of coarser and finer stripes are often observed (see Photo 1), which is here termed "longitudinal stripes of sorting." Such a bed condition promotes a transverse secondary flow from the rough to smooth parts near the bed . Particularly when the transverse wave length of sorting is roughly twice the flow depth, cellular secondary currents often called longitudinal vortices develop and maintain themselves (Müller & Studerus (7), Nakagawa et al.(8)).

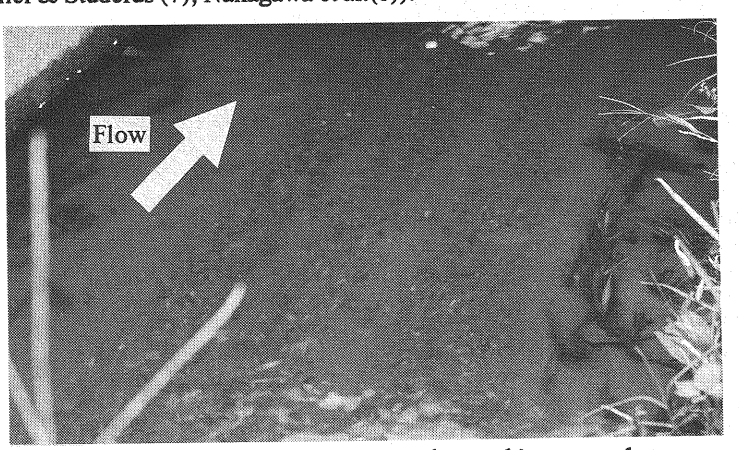

Photo 1 Longitudinal sorting stripes observed in a natural stream

Cellular secondary currents and longitudinal sorting stripes are promoted or suppressed each other. Such an interaction between them has been investigated mostly from the view point of secondary current initiation (Müller & Studerus (7), Nakagawa et al.(8)) but scarcely from the view point of mechanics of graded material transport. In this paper, the formation mechanism of the longitudinal stripes of sorting is investigated from the view point of selective transport properties of graded bed-material, and the equilibrium stripes are predicted.

Müller & Studerus (7) and Nakagawa et al. (8) made artificial longitudinal stripes of different roughness in order to produce a lateral inhomogeneity of bed shear stress and successively cellular secondary currents, and conducted detailed measurements of such stable cellular currents. According to their experiments, lateral secondary-flow component, the intensity of which near the bottom is 2~5% of the maximum main-flow velocity, was confirmed. Such secondary currents often bring longitudinal stripes of bed undulation often called "sand ribbons" or "sand ridges," and a few theoretical analysis on their formation mechanism (Kuroki & Kishi (5)) and several experimental studies, mainly turbulence measurements, were conducted (Hirano & Ohmoto (4), Nezu et al. (12)).

In this paper, the formation of longitudinal stripes of sorting is treated in terms of an instability of spanwise distribution of bed-surface composition. The longitudinally alternate sorting often called diffuse gravel sheet was also analyzed as an instability problem (Tsujimoto & Motohashi (15)), for which a linear analysis was performed.

OUTLINE FOR FORMATION MECHANISM OF LONGITUDINAL STRIPES WITH SORTING

A secondary current has a lateral component from a relatively rough part ((A) region in Fig. 1), where coarser particles dominantly exist, to a relatively smooth part ((B) region in Fig. 1), and it causes lateral sediment transport from a rough part to a smooth part. Finer particles are picked-up more from the bed but are transported in shorter distance compared with coarser particles, and thus, the difference of bed-surface composition is sometimes amplified (unstable) but sometimes suppressed (stable). By describing the bed-load transport behavior, the condition of instability of bed-surface composition can be clarified, and it corresponds to the condition that the sorting stripes exists. When the difference of bed-surface composition is promoted, the cellular secondary currents grow to be stable.

Even when the lateral sorting develops initially, the selective transport diminishes the number of the fine particles exposed at the bed surface in a rough stripe ((A) region) and it ceases increasingly to produce equilibrium sorting stripes.

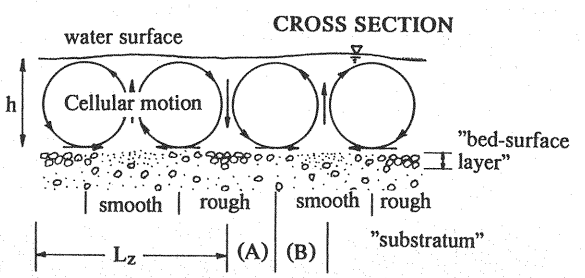

Fig. 1 Front view of cellular secondary current and longitudinal sorting stripes

In the following, based on the above phenomenological understanding, an analytical model is proposed to clarify the criterion of longitudinal stripes of sorting and the spanwise distributions of bed-surface composition and sediment transport rate for the equilibrium longitudinal stripes with sorting.

BED-LOAD TRANSPORT MODEL OF GRADED MATERIAL

In order to describe non-equilibrium or selective transport of graded material and subsequent sorting process, a model constituted by pick-up rate and step length for each grain size is a powerful means. In this chapter, the framework of the model of graded material transport and the evaluation of the constituent parameters are investigated.

Sediment Pick-Up

The pick-up rate of bed-material particles for each grain size can be estimated by applying the formula derived by Nakagawa & Tsujimoto (9) with a modification of the critical tractive force, as follows:

$$p_{si*} \equiv p_{si}\sqrt{d_i/(\sigma/\rho-1)g} = F_0\tau_{*i}(1-k_2\tau_{*ci}/\tau_{*i})^m \qquad (1)$$

in which p_{si}=pick-up rate for each grain size; d_i=diameter of sediment particle belonging to the i-th fraction; $\tau_{*i}=u_*^2/[(\sigma/\rho-1)gd_i]$; τ_{*ci}=dimensionless critical tractive force for each grain size of heterogeneous bed material; u_*=shear velocity; σ=mass density of sediment; ρ=mass density of fluid; g=gravity acceleration; and the empirical parameters are determined as follows: $F_0=0.03$; $k_2=0.7$; and $m=3$ (Nakagawa & Tsujimoto (9)).

The ratio of the dimensionless critical tractive force for each grain size of mixture, τ_{*ci}, to that for sand of the mean diameter in the mixture, τ_{*cm}, is expressed as a function of (d_i/d_m), and Egiazaroff's formula (2) somewhat modified by Ashida & Michiue (1) for finer materials is often applied, which are written as follows:

$$\tau_{*ci}/\tau_{*cm} = \begin{cases} \{\ln 19/\ln[19(d_i/d_m)]\}^2 & (d_i/d_m>0.4) \\ 0.85/(d_i/d_m) & (d_i/d_m\le 0.4) \end{cases} \qquad (2)$$

However, the above formula overestimates the difference of the critical tractive force due to sediment size in the mixture as suggested by a force-balance analysis on a bed with an irregularity of the order of sediment diameter (Nakagawa et al. (11)) or by data analysis for paved bed (Parker et al. (13)) and for dynamic equilibrium bed (Michiue & Suzuki (6)). Then, the following formula is appropriate to describe the relation between τ_{*ci}/τ_{*cm} and d_i/d_m instead of Eq. 2:

$$\tau_{*ci}/\tau_{*cm} = (d_i/d_m)^{-1} \qquad (3)$$

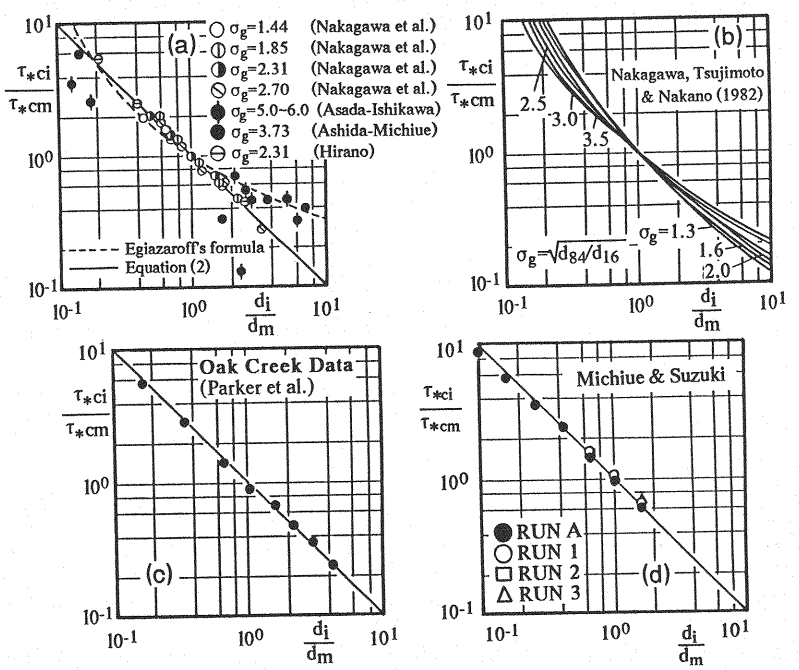

Fig. 2 Critical tractive force for each grain size of sediment mixture

The previous data are plotted in Fig. 2(a) with Eqs. 2 and 3. As a reference, the results by Nakagawa et al. (11), Parker et al. (13), and Michiue & Suzuki (6) are also shown in Figs. 2(b)~(d). Although it is difficult to judge the superiority between Eqs. 2 and 3, Eq. 3 is adopted here because of its mathematical simplicity. According to Eq. 3, particles belonging to any fraction of size have the same threshold of mobility, but it does not conclude no selective transport process (see Eq. 5). The ratio of τ_{*cm} to the dimensionless critical tractive force for uniform sand ($\tau_{*c0}\cong 0.05$ when the grain-size Reynolds number is larger than almost 100), α_{cm}, might be a function of gradation of sediment mixture (Nakagawa et al. (11)). Then, Eq. 1 is reduced to

$$p_{si*} \equiv p_{si}\sqrt{d_i/(\sigma/\rho-1)g} = F_0\alpha_{cm}\tau_{*c0}\eta_m(1-k_2/\eta_m)^m(d_i/d_m)^{-1} \tag{4}$$

in which $\eta_m \equiv \tau_{*m}/\tau_{*cm}$; and the subscript m indicates the value for the fraction with the mean diameter in the mixture. In Fig. 3(a), the previous data are plotted with Eq. 4 (Eq. 1 with Eq. 3). As a reference, the evaluation of the pick-up rate by Eq. 1 with Eq. 2 is compared with the data in Fig. 3(b) (Nakagawa et al. (10), (11)). When Eq. 4 is adopted, the following relation is derived:

$$p_{si}/p_{sm} = (d_i/d_m)^{-3/2} \tag{5}$$

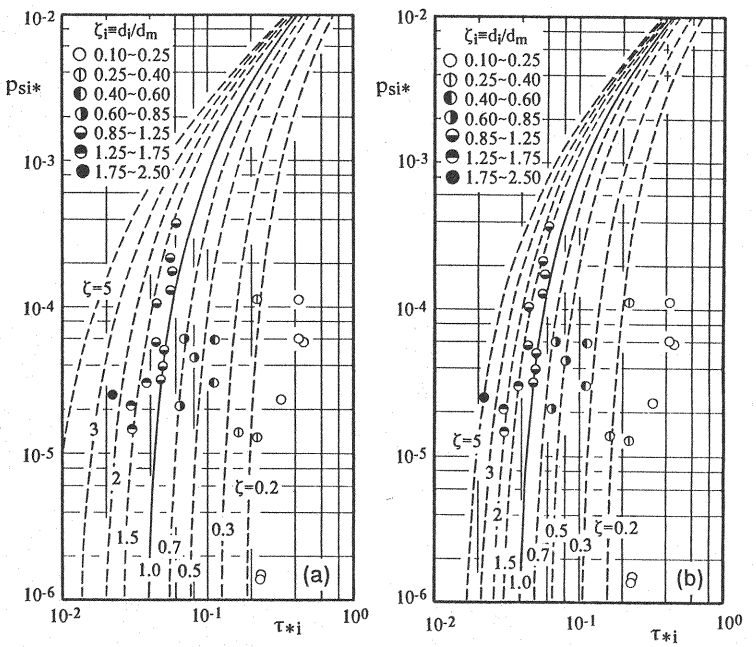

Fig. 3 Pick-up rate for each grain size of sediment mixture

Lateral Transport of Sediment

The experimental data indicate that the step length for each grain size of mixture follows an exponential distribution, the average of which (Λ_i) is 20~50 times each grain size (Nakagawa et al. (11)). In the present situation, the lateral component of flow velocity induces lateral sediment transport from the stripe (A) to (B) (see Fig. 4). If the transverse bed slope is negligible, the lateral component of step length is expressed as a product of the step length and $\Gamma \equiv \tan\gamma$, in which γ=deflection angle of flow near the bed from the longitudinal direction. Although Γ changes spatially, its detailed behavior is not yet clear, and thus here it is assumed to be constant. However, the fact that the movement of sediment is restricted in the stripes (A) and (B) should be taken into account.

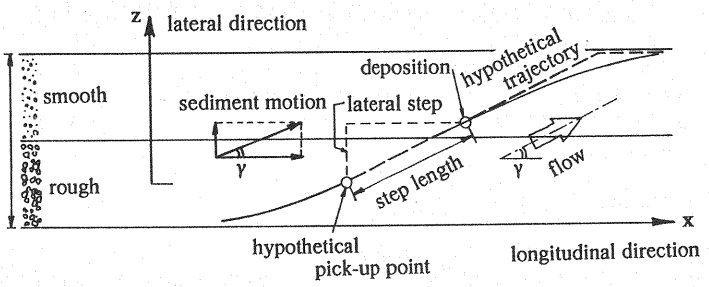

Fig. 4 Schematic figure of lateral bed-load transport

Then, the probability that a particle of diameter d_i dislodged from the stripe (A) reaches the stripe (B), p_{Ti}, can be approximately calculated as follows (see Fig. 3):

$$p_{Ti} = \int_{L_z/8}^{\infty} f_{Zi}(z)dz = \int_{L_z/8}^{\infty} \frac{1}{\Lambda_i \Gamma} \exp\left(-\frac{z}{\Lambda_i \Gamma}\right) dz = \exp\left(-\frac{L_z}{8\Lambda_i \Gamma}\right) \tag{6}$$

in which Γ is defined at the boundary of the two stripes and thus it is a transversally maximum of Γ; and $f_{Zi}(z)$=probability density function of lateral component of the step length and an exponential distribution is here reasonably assumed. The probability that $z>3L_z/8$ has been sophisticatedly concentrated at $z=3L_z/8$ because sediment cannot be transported beyond the other edge of the stripe (B). Eq. 6 provides the following relation:

$$\frac{p_{Ti}}{p_{Tm}} = \exp\left[-\frac{L_z}{8\Lambda_i \Gamma}\left(\frac{d_m}{d_i} - 1\right)\right] \tag{7}$$

Then, the volume of sediment for each grain size transported from the stripe (A) to (B) per unit time per unit longitudinal length, V_i, is written as follows:

$$\frac{V_i}{V_m} = \frac{p_{si}}{p_{sm}} \frac{p_{Ti}}{p_{Tm}} = \left(\frac{d_i}{d_m}\right)^{-3/2} \exp\left[-\frac{L_z}{8\Lambda_i \Gamma}\left(\frac{d_m}{d_i} - 1\right)\right] \tag{8}$$

Furthermore, the transport discharge distributes transversally on a bed with longitudinal stripes of sorting. The bed load dislodged from the stripe (A) partially contributes the transport rate on the stripes (A) and (B), q_{BiAA} and q_{BiBA}, respectively; while all the bed load dislodged from the stripe (B) contributes the transport rate on the stripe (B), q_{BiBB}. The transport rates of the stripe (A) and (B), q_{BiA} and q_{BiB}, are expressed as follows:

$$q_{BiA}=q_{BiAA}\ ; \qquad q_{BiB}=q_{BiBA}+q_{BiBB} \tag{9}$$

$$q_{BiAA}=(1-\rho_0)\theta_{EPiA}\, p_{siA} \int_0^{L_z/8} \int_{\zeta}^{\infty} f_{Xi}(z)dz\, d\zeta$$

$$= (1-\rho_0)\theta_{EPiA}\, p_{siA}\, \Lambda_i \left[1-\exp\left(-\frac{L_z}{8\Lambda_i \Gamma}\right)\right] \tag{10}$$

$$q_{BiBA}=(1-\rho_0)\theta_{EPiA}\, p_{siA} \int_{L_z/8}^{\infty} \int_{\zeta}^{\infty} f_{Xi}(z)dz\, d\zeta\, f_{Xi}(z)dz)\, d\zeta$$

$$= (1-\rho_0)\theta_{EPiA}\, p_{siA}\, \Lambda_i \exp\left(-\frac{L_z}{8\Lambda_i \Gamma}\right) \tag{11}$$

in which θ_E=thickness of the bed-surface layer ("exchange" layer (3)); and ρ_0=porosity of bed material.

CRITERION FOR OCCURRENCE OF SORTING STRIPES

In the present model, the bed material is composed of two typical size particles (sand and gravel) of which diameter are d and βd, respectively (β>1). When the volumetric ratio of the coarser material in the bed-surface layer (sometimes called a layer of "exchange") is p, the (hypothetical) mean diameter of bed-surface layer is written as follows:

$$d_m = [(1-p)+\beta p]d \tag{12}$$

d_m or p is a representative parameter of each stripe of sorting.

For simplicity, two stripes (A) and (B) (see Fig. 1) are considered, and the volumetric ratio of the coarser material in the bed-surface layers of (A) and (B) stripes are expressed as p_A and p_B, respectively, by neglecting a continuous change of p from (A) to (B). Moreover, it is here assumed that the difference of the bed shear stress between the stripe (A) and (B) is negligible. Thus, the difference of sediment pick-up from the bed between (A) and (B) is assumed to be caused only by the difference of the bed-surface composition between (A) and (B).

In the present model, it is assumed that the bed material is transported from the stripe (A) to (B) by the resultant flow near the bottom defined at the boundary between (A) and (B) (deflection angle is γ). As a result, the volumetric ratio, r_C, of the coarser material to the total sediment transported from the stripe (A) to (B) is calculated from Eq. 8 as follows:

$$r_C = \frac{p_A\beta^{-3/2}\exp[L^*(1-1/\beta)]}{1-p_A+p_A\beta^{-3/2}\exp[L^*(1-1/\beta)]} \tag{13}$$

in which $L^*\equiv L_z/(8\Lambda\Gamma)$; Λ=mean step length of the finer material; and the subscripts A and B indicate the values for the stripe (A) and (B). The secondary flow induced by such a difference of bed roughness yields the maximum lateral flow velocity of the order of 2~5% of the maximum main velocity (4, 7, 11). Since the longitudinal velocity near the bottom is the order of about 30% of the maximum main flow velocity, the deflection γ of the near-bed flow from the longitudinal direction is approximately estimated to be $\Gamma\equiv\tan\gamma\cong 0.1$.

When the volumetric ratio of the coarser material to the total sediment transported from the region (A) to (B), r_C, is smaller than the volumetric ratio of the coarser material to the total material in the bed-surface layer of the region (B), p_B, the lateral distribution of bed-surface composition is unstable, and the sorting stripes grow. The criterion of the initial occurrence of such an instability is given under the condition that $p_A=p_B$, and it is written as follows:

$$M^*(\beta) \equiv \beta^{-3/2}\exp[L^*(1-1/\beta)] < 1.0 \tag{14}$$

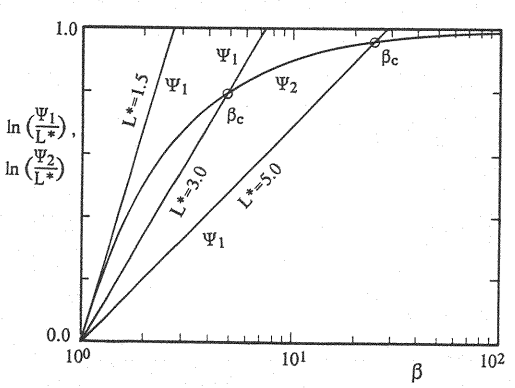

Fig. 5 Determination of neutral instability of lateral alternate sorting

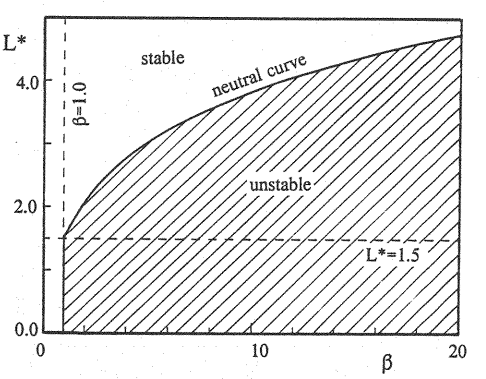

Fig. 6 Unstable region for lateral alternate sorting

The relation between $\ln(\Psi_1/L^*)$ and $\ln(\Psi_2/L^*)$ is depicted in Fig. 5, in which $\Psi_1 \equiv \exp[L^*(1-1/\beta)]$ and $\Psi_2 \equiv \beta^{3/2}$, and it reveals that the neutral instability (which corresponds to the intersection of the two curves in Fig. 5) is given as a combination of β and L^* as shown in Fig. 6. Since it is expected that $L_z \cong 2h$ (h=flow depth), $\Lambda/d \cong 30$, and $\Gamma \cong 0.1$, thus $L^* \cong (h/d)/10$. Under the condition of the same value of L^* or (h/d), the longitudinal sorting stripes are more easily formed for the larger value of the ratio of the diameter of the coarser material to that of the finer material (β), independently of the bed shear stress and the volumetric ratio of the coarser material to the total material in the substratum.

EQUILIBRIUM STRIPES OF SORTING

With the progress of lateral sorting, the difference between p_A and p_B increases, and the condition for development of lateral sorting deduced under the assumption that $p_A=p_B$ falls no longer valid. Phenomenologically, the decrease in the number of fine particles exposed at the rough stripe (A) suppresses the transport of fine material to the stripe (B), and sorting process no longer goes on.

The changes of p_A and p_B with the progress of sorting are here represented by a dimensionless parameter ψ_p as follows:

$$p_A=p_0(1+\psi_p) \; ; \qquad p_B=p_0(1-\psi_p) \tag{15}$$

in which p_0=initial volumetric ratio of the coarser material in the surface layer (volumetric ratio of the coarser material in the substratum). Then, the criterion for instability of the bed-surface composition is written as follows, instead of Eq. 14:

$$M^*(\beta) < \xi(p_0,\psi_p) \tag{16}$$

in which

$$\xi(p_0,\psi_p) \equiv 1- \frac{2\psi_p}{(1+\psi_p)[1-p_0(1-\psi_p)]} \tag{17}$$

Eq. 14 is identified with Eq. 16 with $\xi=1.0$, because $\psi_p=0$ for the initial stage.

With the progress of sorting, ξ decreases, and the unstable region of bed-surface composition in the L^*~β plane is increasingly suppressed as illustrated in Fig. 7. This behavior explains the existence of the equilibrium state of sorting, as follows: When the hydraulic condition (h/d) and the ratio of the diameter of gravel and that of sand, β, are given, a point K is determined on the L^*~β plane as shown in Fig. 7. If the point K belongs to the initially unstable region which is below the neutral curve for $\xi=1.0$, the longitudinal stripes of sorting develop. With the progress of sorting, ξ decreases and the sorting process reaches its equilibrium when ξ becomes the value ξ_e so as the point K is just on the neutral curve determined by ξ_e.

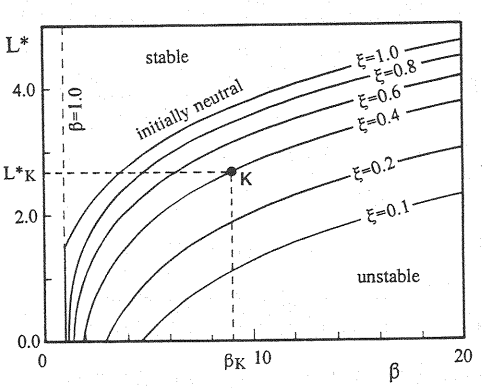

Fig. 7 Change of instability condition with progress of sorting

When L* and β are given, the value of ξ for equilibrium, ξ_e, is calculated as follows:

$$\xi_e=\beta^{-3/2}\exp[L^*(1-1/\beta)] \tag{18}$$

The value of ψ_p for equilibrium, ψ_{pe}, is obtained as a solution of the following equation which satisfies the condition that $0<\psi_{pe}<1.0$:

$$\xi_e= 1- \frac{2\psi_{pe}}{(1+\psi_{pe})[1-p_0(1-\psi_{pe})]} \tag{19}$$

The solution is obtained as follows:

$$\psi_{pe} = \frac{1+\xi_e-\sqrt{D_e}}{2p_0(1-\xi_e)} \tag{20}$$

in which D_e is described by

$$D_e \equiv [1-4p_0(1-p_0)](1-\xi_e)^2+4\xi_e \tag{21}$$

When ψ_{pe} is obtained, the volumetric ratios of the coarser material and the mean diameters of the bed-surface layer of the regions (A) and (B), p_{Ae}, p_{Be}, d_{mAe} and d_{mBe}, are clarified, as follows:

$$p_{Ae}=p_0(1+\psi_{pe}) \; ; \qquad p_{Be}=p_0(1-\psi_{pe}) \tag{22}$$

$$\frac{d_{mAe}}{d} = 1+ \frac{(\beta-1)p_0\psi_{pe}}{(\beta-1)p_0+1} \; ; \quad \frac{d_{mBe}}{d} = 1- \frac{(\beta-1)p_0\psi_{pe}}{(\beta-1)p_0+1} \; ; \quad \frac{d_{mAe}}{d_{mBe}} = \frac{(\beta-1)p_0(1+\psi_{pe})+1}{(\beta-1)p_0(1-\psi_{pe})+1} \tag{23}$$

in which the subscript e indicates the values of equilibrium sorting stripes.

In Fig. 8, the equilibrium volumetric ratio of the coarser material in the surface layer of the region (A), p_{Ae}, are shown against β with p_0 and L* as parameters. Moreover in Fig. 9, the difference of the mean diameters between the stripe (A) and (B) under the equilibrium is demonstrated.

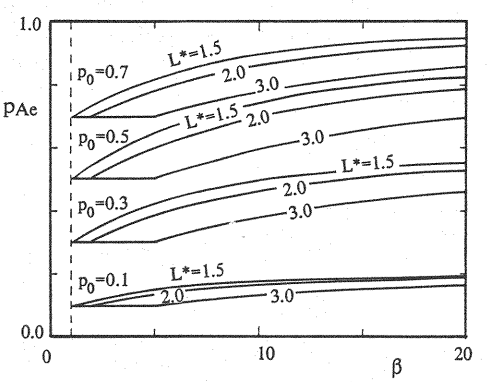

Fig. 8 Bed-surface composition of equilibrium stripes of sorting

Under the equilibrium conditions, the ratio of the transport rate in a "smooth" stripe (q_{BAe}) to that in a "rough" stripe (q_{BBe}) is calculated from Eqs. 9~11, as follows:

$$\frac{q_{BiBe}}{q_{BiAe}} = \frac{(1+\psi_{pe})\exp[-L_z/(8\Lambda_i\Gamma)]+(1-\psi_{pe})(p_{siB}/p_{siA})}{(1+\psi_{pe})\{1-\exp[-L_z/(8\Lambda_i\Gamma)]\}} \tag{24}$$

Eq. 4 suggests that $p_{siB}/p_{siA}=(d_{mB}/d_{mA})$. Hence,

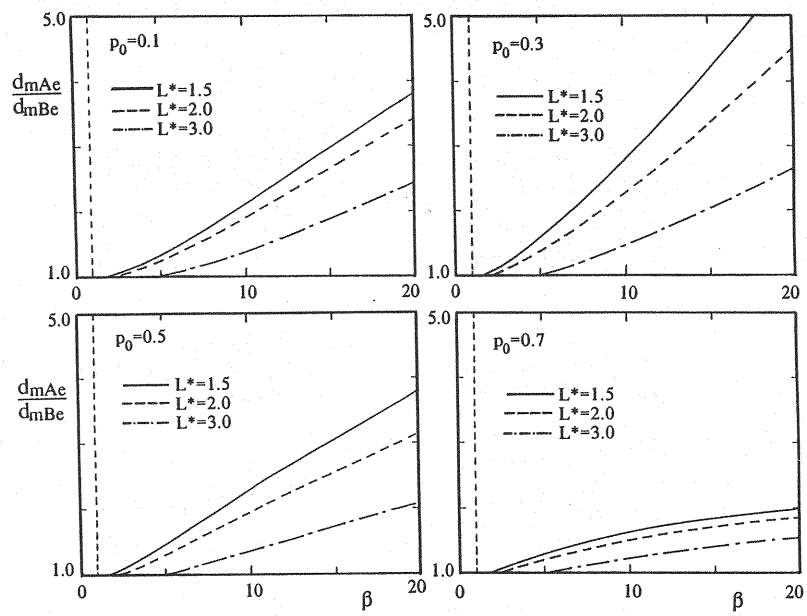

Fig. 9 Mean diameter of bed-surface of equilibrium stripes of sorting

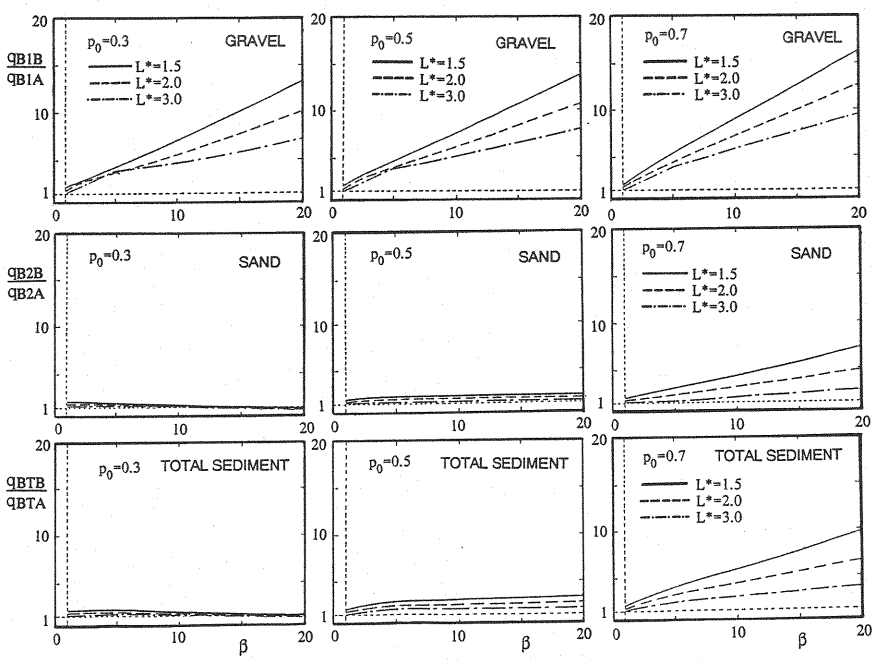

Fig. 10 Total and fractional bed-load transport rate on equilibrium sorting stripes

$$\frac{q_{BiBe}}{q_{BiAe}} = \frac{(1+\psi_{pe})\exp[-L_z/(8\Lambda_i\Gamma)]+(1-\psi_{pe})(d_{mB}/d_{mA})}{(1+\psi_{pe})\{1-\exp[-L_z/(8\Lambda_i\Gamma)]\}} \quad (25)$$

The fractional and total bed-load transport rates on the equilibrium sorting stripes are calculated and some examples are shown in Fig.10. The coarser material transport on the stripe A always increases with β, but the finer material transport on the stripe A increases with β only when the sorting stripes appreciably develops. The total sediment transport is eventually affected by predominant sediment fraction. Unfortunately, we have no available data up to now to compare with the above theoretical results.

CONCLUSIONS

In streams composed of sand and gravel, we often observe longitudinal stripes of alternate lateral sorting and cellular secondary currents. They are promoted or suppressed with each other through an interaction between them. In this paper, such an interaction has been investigated mainly from the view point of mechanics of bed-load transport of heterogeneous size material (or graded material) affected by secondary current.

A secondary current brings about a lateral bed-load transport from a "rough" stripe to a "smooth" stripe, and alternate sorting develops when the finer material is predominantly transported laterally. A transport model constituted by pick-up rate and step length for each grain size has been prepared and the mechanics of lateral sorting has been described. Based on it, a criterion of occurrence of longitudinal stripes of sorting has been clarified. By considering the decrease of the finer material exposed in the "rough" stripe with the progress of sorting, the equilibrium stripes have been analytically investigated. The spanwise distribution of the bed roughness and bed-load transport rate for equilibrium longitudinal stripes of sorting have been predicted.

Some assumptions have been imposed to simplify the present analysis in this study. Actually, the boundary shear stress must have a transverse distribution on sorting stripes, and the amplitude of secondary currents may change with the progress of sorting. The detailed measurements of flow and fractional sediment transport on beds with lateral sorting will refine the present model.

The most part of this paper is translated from the author's preceding paper (14) written in Japanese, some part of which is revised herein.

REFERENCES

1. Ashida, K. and M. Michiue : Studies on bed load transportation for nonuniform sediment and river bed variation. Annuals, Disaster Prevention Research Institute, Kyoto University, No.14B, pp.259-273, 1971 (in Japanese).
2. Egiazaroff, I.V. : Calculation of nonuniform sediment concentration. Journal of the Hydraulics Division, ASCE, Vol.91, HY4, pp.73-80, 1965.
3. Hirano, M. : River bed degradation with armoring. Proc. JSCE, No.207, pp.51-60, 1971 (in Japanese).
4. Hirano, M. and T. Ohmoto : Experimental study on the interaction between longitudinal vortices and sand ribbons. Proc. 6th Congress of APD-IAHR, Kyoto, Japan, Vol.II, pp.59-66, 1988.
5. Kuroki, M. and T. Kishi : Sediment transport and dispersion of pollutant in flow with longitudinal vortices. Proc. 25th Japanese Conference on Hydraulics, JSCE, pp.433-438, 1981 (in Japanese).
6. Michiue, M. and K. Suzuki : Sediment discharge of nonuniform sand bed during increase and decrease periods of flood discharge. Proc. JSCE, No.399, II-10, pp.95-103, 1988 (in Japanese).
7. Müller, A. and X. Studerus : Secondary flow in an open channel. Proc. 18th Congress of IAHR, Cagliari, Italy, Paper B.a.3, pp.142-144, 1979.
8. Nakagawa, H., I. Nezu and A. Tominaga : Turbulent structure with and without cellular secondary currents over various bed configurations. Annual, Disaster Prevention Research Institute, Kyoto University, No.24B-2, pp.315-338, 1981 (in Japanese).
9. Nakagawa, H. and T. Tsujimoto : Sand bed instability due to bed load motion. Journal of the Hydraulics Division, ASCE, Vol.106, HY12, pp.1029-1051, 1980.
10. Nakagawa., T., T. Tsujimoto and T. Hara : Armoring in alluvial bed composed of sediment mixtures. Annuals, Disaster Prevention Research Institute, Kyoto University, No.20B-2, pp.355 370, 1977 (in Japanese).

11. Nakagawa, H., T. Tsujimoto and S. Nakano : Characteristics of sediment motion for respective grain sizes of sand mixtures. Bulletin, Disaster Prevention Research Institute, Kyoto university, Vol.32, pp.1-32, 1982.
12. Nezu, I., H. Nakagawa and N. Kawashima : Cellular secondary currents and sand ribbons in fluvial channel flows. Proc. 6th Congress of APD-IAHR, Kyoto, Japan, Vol.II, pp.51-58, 1988.
13. Parker, G., P.C. Klingeman and D.G. McLean : Bedload and size distribution in paved gravel-bed streams. Journal of the Hydraulics Division, ASCE, Vol.108, HY4, pp.544-571.
14. Tsujimoto, T. : Formation of longitudinal stripes due to lateral sorting by cellular secondary currents. Proc. 33rd Japanese Conference on Hydraulics, JSCE, pp.403-408, 1989 (in Japanese).
15. Tsujimoto, T. and K. Motohashi : Formation mechanism and predominant wave length of alternate longitudinal sorting on a stream bed composed of sand and gravel. Proc. 33rd Japanese Conference on Hydraulics, JSCE, pp.409-414, 1989 (in Japanese).

APPENDIX - NOTATION

The following symbols are used in this paper:

d	= diameter of sand (finer material);
d_i	= diameter of the i-th fraction sediment;
d_m	= mean diameter;
$f_{Zi}(z)$	= probability density of lateral component of step length for each grain size in sediment mixture;
F_0	= constant in pick-up rate formula;
g	= gravitational acceleration;
h	= flow depth;
k_2	= constant in pick-up rate formula;
L_z	= transverse wave length of sorting stripes;
L^*	= dimensionless wave length ($\equiv L_z/(8\Lambda\Gamma)$);
m	= constant in pick-up rate formula;
M^*	= index of instability defined by Eq. 14;
p	= volumetric ratio of coarser material to the total material in the bed-surface layer;
p_0	= volumetric ratio of coarser material to the total material in the substratum;
p_i	= volumetric ratio of the i-th fraction material in the bed-surface layer;
p_{si}	= pick-up rate for each grain size;
p_{s*}	= dimensionless pick-up rate ($\equiv p_s\sqrt{d/(\sigma/\rho-1)g}$);
p_{Ti}	= probability that a particle of the i-th fraction dislodged from stripe A reaches B.
q_{Bi}	= bed-load transport rate for each grain size;
r_C	= volumetric ratio of coarser material to the total transported from stripe A to B;
u_*	= shear velocity of main-flow direction;
V_i	= volume of sediment for each grain size transported from stripe A to B;
z	= transverse coordinate;
α_{cm}	$\equiv \tau_{*cm}/\tau_{*c0}$;
β	= ratio of diameter of gravel (coarser material) to sand (finer material);
γ	= deflection angle of flow near the bottom from the longitudinal direction;
Γ	$\equiv \tan\gamma$;
η_m	$\equiv \tau_{*m}/\tau_{*cm}$;

θ_E = thickness of bed-surface ("exchange") layer;
Λ = mean step length of sand (fine material);
Λ_i = mean step length for each grain size;
ξ = index to express the progress of sorting defined by Eq. 17;
ρ = mass density of fluid;
ρ_0 = porosity of bed material;
σ = mass density of sediment;
τ_{*c0} = dimensionless critical tractive force for uniform bed material;
τ_{*ci} = dimensionless critical tractive force for each grain size;
τ_{*cm} = dimensionless critical tractive force for sediment of mean diameter in mixture;
τ_{*i} = dimensionless tractive force for each grain size ($\equiv u_*^2/[(\sigma/\rho-1)gd_i]$);
Ψ_p = index of sorting defined by Eq. 15;
Ψ_1 $\equiv \exp[L^*(1-1/\beta)]$; and
Ψ_2 $\equiv \beta^{3/2}$.

Subscripts

e = equilibrium states; and
A, B = stripe A and stripe B, respectively.